

# Hysteresis and synchronization processes of Kuramoto oscillators on high-dimensional simplicial complexes with the competing simplex-encoded couplings

Malayaja Chutani<sup>1</sup>, Bosiljka Tadić<sup>2,3</sup>, and Neelima Gupte<sup>1,4</sup>

<sup>1</sup>*Department of Physics, Indian Institute of Technology Madras, Chennai 600036, India*

<sup>2</sup>*Department of Theoretical Physics, Jožef Stefan Institute, Jamova 39, Ljubljana, Slovenia*

<sup>3</sup>*Complexity Science Hub Vienna - Josephstadter Strasse 39, Vienna, Austria and*

<sup>4</sup>*Complex Systems and Dynamics Group, Indian Institute of Technology Madras, Chennai 600036, India*

(Dated: June 9, 2021)

Recent studies of dynamic properties in complex systems point out the profound impact of hidden geometry features known as simplicial complexes, which enable geometrically conditioned many-body interactions. Studies of collective behaviours on the controlled-structure complexes can reveal the subtle interplay of geometry and dynamics. Here, we investigate the phase synchronisation (Kuramoto) dynamics under the competing interactions embedded on 1-simplex (edges) and 2-simplex (triangles) faces of a homogeneous 4-dimensional simplicial complex. Its underlying network is a 1-hyperbolic graph with the assortative correlations among the node's degrees and the spectral dimension that exceeds  $d_s = 4$ . By solving numerically the set of coupled equations for the phase oscillators associated with the network nodes, we determine the time-averaged system's order parameter to characterise the synchronisation level. In the absence of higher interactions, the complete synchrony is continuously reached with the increasing positive pairwise interactions ( $K_1 > 0$ ), and a partial synchronisation for the negative couplings ( $K_1 < 0$ ) with no apparent hysteresis. Similar behaviour occurs in the degree-preserved randomised network. In contrast, the synchronisation is absent for the negative pairwise coupling in the entirely random graph and simple scale-free networks. Increasing the strength  $K_2 \neq 0$  of the triangle-based interactions gradually hinders the synchronisation promoted by pairwise couplings, and the non-symmetric hysteresis loop opens with an abrupt desynchronisation transition towards the  $K_1 < 0$  branch. However, for substantial triangle-based interactions, the frustration effects prevail, preventing the complete synchronisation, and the abrupt transition disappears. These findings shed new light on the mechanisms by which the high-dimensional simplicial complexes in natural systems, such as human connectomes, can modulate their native synchronisation processes.

## I. INTRODUCTION

In complex systems, collective dynamics is a marked signature of emerging properties related to complex structure, studied by mapping onto networks [1]. The synchronisation of oscillator systems is a paradigmatic stochastic process for study the emergence of coherent behaviour in many natural and laboratory systems [2]. In recent years, research focuses on the system's hidden geometry features [3, 4] and their impact on dynamics. Notably, new dynamical phenomena appear that can be related to the higher-order connectivity and interactions supported by the system's hidden geometry, which is mathematically described by simplicial complexes [5–11].

A formal theory of the simplicial complexes of graphs [12–14] defines a simplicial complex as a structure consisting of different simplexes, e.g.,  $n$ -cliques, which share one or more common nodes representing a geometrical face of the implicated simplexes. For example, an  $n$ -clique is a full graph of  $n$  nodes, and its faces are simplexes of the order  $q = 0, 1, 2, 3, \dots, q_{max}$ , where  $q_{max} = n - 1$  defines the dimension of the simplex. Hence, the dimension of the simplicial complex is defined by order of the largest simplex that it contains. Recent studies revealed simplicial architecture in networks mapping many complex systems from the brain [15–18], designed materials [19] and physics problems [20–23], to structures emerging from online social endeavours [24] and large-scale social networks [25, 26]. Such simplicial struc-

ture naturally underlies many-body interactions [6]. However, revealing the mechanisms by which such high-dimensional simplicial complexes determine collective dynamics in these complex systems represents a challenging problem.

In this context, the generative models of high-dimensional simplicial complexes of a controlled structure are of great importance [27–30]. For example, in the model of self-assembly of cliques of different size developed in Ref. [27], the assembly is controlled by two factors. These are the geometric compatibility of the attaching clique's faces with the once already built-in the growing structure, and the chemical affinity towards the addition of new nodes. Varying the chemical affinity, one can grow different structures from sparsely connected cliques that share a single node to the very dense structure of large clique sharing their most prominent sub-clique, see the online demo on [29]. Moreover, the architecture of simplicial complexes manifests on several unique properties of the underlying network (1-skeleton of the simplicial complex), that can affect the pairwise interaction, see section II for details. For example, the network's spectral dimension can vary from the values close to the tree graphs in sparsely connected cliques of any size, to the values  $d_s \geq 4$ , in the case of large densely connected cliques, as shown in Ref. [31]. Hence, the structure–dynamics interplay can be expected both because of the pairwise and higher-order interactions due to the actual architecture of simplicial complexes. More precisely, it has been demonstrated by studies of spin kinetics [7, 8], contagious dynamics [11], and synchronisation processes [9, 10, 32] on var-

ious simplicial complexes. Notably, in the field-driven magnetisation reversal on simplicial complexes [7, 8], the antiferromagnetic interactions via links of the triangle faces provide strong geometric frustration effects that determine the shape of the hysteresis loop. The higher-order interactions then affect its symmetry, meanwhile the width of the hysteresis remains strictly determined by the dimension of the simplicial complex. In the contagious and synchronisation processes, on the other hand, the appearance of the hysteresis loop is strictly related to the higher-order interactions. The synchronisation has been studied extensively on a variety of networks [2, 33] using an ensemble of 2-dimensional phase oscillators (Kuramoto model) with interactions via network edges. It has been understood that the onset of synchronous behaviour can be affected by the local connectivity and correlations among the nodes [34], and global features captured by the network's spectral dimension [35]. The nature of synchronisation transition can depend on the process' sensitivity to the sign of interactions, time delay, and the frustration effects causing new phenomena [36–41]. Furthermore, the presence of higher-order interactions are shown to induce an abrupt desynchronisation, depending on the dimension of the dynamical variable, and the range of couplings [9, 10]. It remains unexplored how the coincidental interactions of a different order, encoded by the faces of a large simplicial complex, cooperate during the synchronisation processes.

Here, we tackle this problem by numerical investigations of synchronisation and desynchronisation processes among Kuramoto phase oscillators considering the leading interactions based on 1-simplices (edges) and 2-simplices (triangles) as the faces of homogeneous 4-dimensional simplicial complexes. The structure is grown by self-assembly of 5-cliques that preferably share the most extensive face. The underlying graph of this simplicial complex possesses several unique features. These are hyperbolicity, assortative mixing, and a high spectral dimension, allowing complete synchronisation when the positive pairwise interaction is increased. Our results suggest that these geometrical properties, even in the absence of the higher-order interactions, can lead to new states with partial synchronisation, mainly when the pairwise coupling is negative, which can be attributed to frustration. Furthermore, these simplex-based interactions have competing effects, leading to different patterns of synchronisation and desynchronisation. Remarkably, the triangle-based interactions tend to hinder the synchronisation processes promoted by the increasing pairwise coupling, leading to the hysteresis loop and the abrupt desynchronisation when the fully synchronised state can be reached, i.e., for a moderate strength of interaction. Both the complete synchrony and the abrupt desynchronisation disappear for strong triangle-based interactions, suggesting the dominance of geometric frustration.

In section II, we present the relevant details of the structure of the simplicial complex and the underlying network. Section III introduces the dynamical model with the simplex-based interactions and discusses the case with pairwise interaction alone. In section IV, the effects of the triangle-based interactions on the order-parameter and hysteresis loop are shown. Section V presents a summary and discussion of the results.

## II. NETWORK GEOMETRY UNDERLYING SYNCHRONISATION PROCESSES

As mentioned in the Introduction, we use the algorithm of cooperative self-assembly introduced in ref. [27, 29] to grow a simplicial complex (SC) by an assembly of 5-cliques. The geometric compatibility of its faces determines the attachment rules of a new clique to the growing structure with the currently built-in cliques; besides, the chemical affinity parameter  $\nu$  modulates the probability of binding along a  $q$ -dimensional face. Effectively, see [27, 28], the positive affinity parameter, as we used here  $\nu = +5$ , lead to the preference of sharing the largest sub-cliques. Thus, the newly added clique mainly consists of a new node and a 4-clique face shared with the previously added clique. An example of the resulting compact structure consisting of 5-cliques is shown in Fig. 1 top-left. To assess the relevance of a particular network property in the observed collective dynamics, we also study the synchronisation of phase oscillators on two randomised versions of our simplicial complex. Specifically, we perform random rewiring that preserves the degree of each node (the network is also shown in Fig. 1 top-right) and a fully randomised structure. For further comparison, we also consider a simple scale-free network with the power-law exponent that coincides with the slope observed in the degree distribution of the SC for the intermediate degree, cf. Fig. 1.

Besides the high spectral dimension of our SC,  $d_s \geq 4$  shown in [31], several other structural measures of these networks relevant to the synchronisation dynamics are given in Fig. 1a-f. Fig. 1e shows that, even though they all contain the same number of nodes ( $q=0$ ) and a similar number of edges ( $q=1$  simplexes), they significantly differ in the presence of higher simplexes. Specifically, a small number of triangles ( $q=2$  simplexes) as the highest structures appear in the entirely random graph. Similarly, the simple scale-free network possesses a small number of triangles and no higher structures. On the other hand, the degree-preserving randomised network still possesses about 30% of the triangles compared to the original simplicial complex and a few tetrahedrons ( $q=3$  simplexes). Meanwhile, the number of tetrahedrons and 5-cliques in the original complex is comparable to the number of edges and nodes, respectively. The distribution of the number of triangles in which a given node participates, also known as generalised degree  $k_i^{(2)}$ , of our simplicial complex is shown in the panel (f) of Fig. 1. Besides the four hubs with many triangles attached to them, the remaining part of the distribution obeys an algebraic decay with the increasing  $k_i^{(2)}$ .

At the level of edges, the underlying graph of our simplicial complex exhibits some characteristic features depicted in Fig. 1a-d in comparison with the other three structures. Specifically, it exhibits a wide range of the degree  $k_i \equiv k_i^{(1)}$  with a few large-degree nodes. In the intermediate range, the cumulative degree distribution has a power-law decay with the exponent  $\gamma \sim 1.81 \pm 0.05$ , matched by the generated scale-free network, see Fig. 1a. Naturally, the degree-preserved randomised structure obeys the same degree distribution; meanwhile, the exponentially decaying distribution characterises the fully ran-

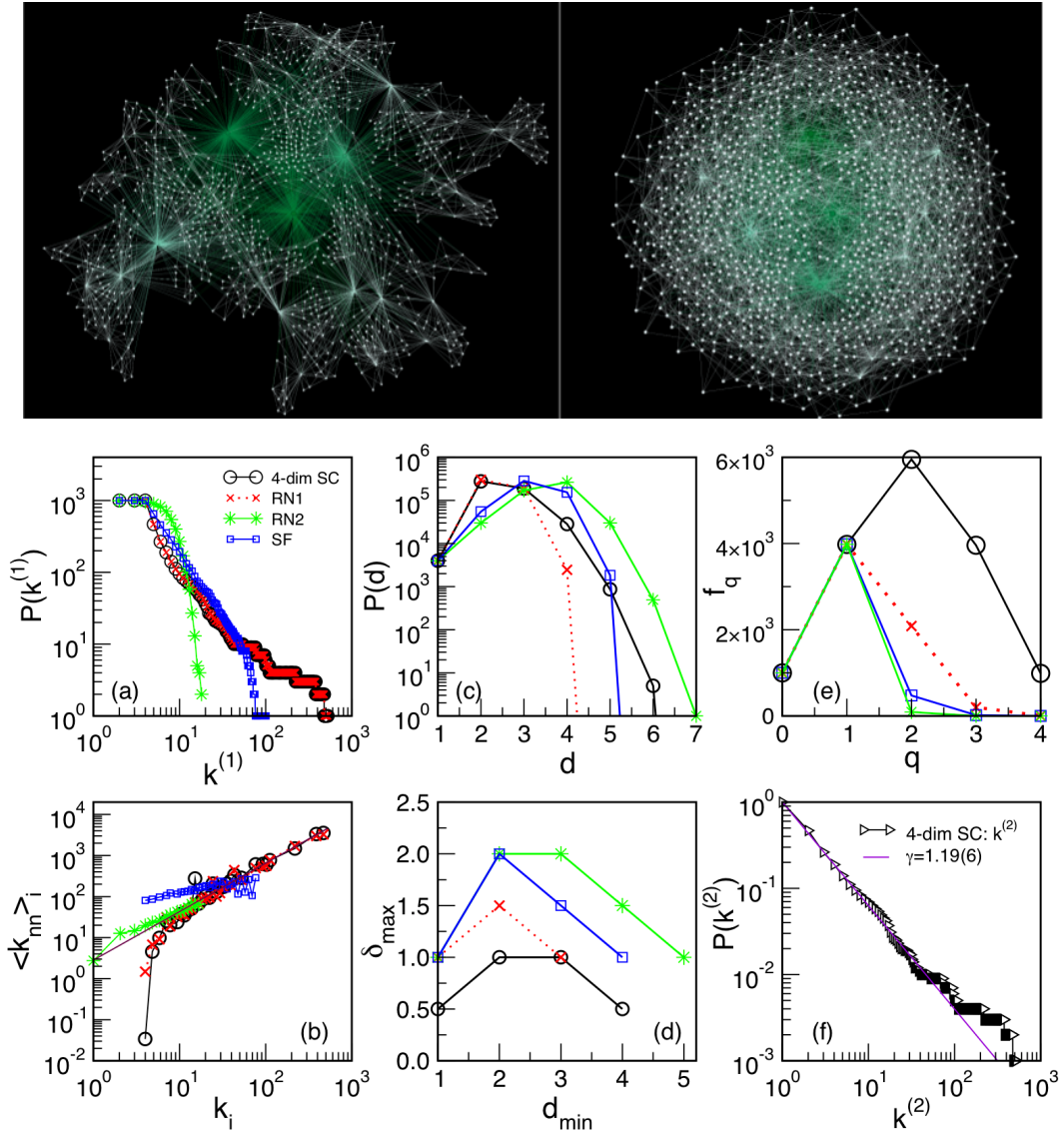


FIG. 1: Visualisation of the homogeneous 4-dimensional simplicial complex SC of 1000 nodes (top, left) and the structure randomised to preserve the nodes degree, RN1 (top, right). Panels a-e show different structural properties, in particular, the cumulative distribution of the node's degree (a), assortativity (b), the distribution of the shortest path distances (c) and the maximum hyperbolicity parameter (d), and the number of faces of different orders  $q = 0, 1, 2, \dots, 4$  up to the maximal cliques (e). Different symbols (colours) are for the original 4-dimensional SC, and the networks of the same size with the degree-preserving randomised structure RN1, the fully randomised structure RN2, and the simple scale-free network with the matching slope, SF. The same legend applies to panels (a-e). Panel (f) shows the normalised distribution of the number of faces per node (generalised degree) in the 4-dimensional SC.

domised structure. Moreover, our network possesses the assortative mixing among the neighbouring node's degree [42]; it is quantified by the positive exponent  $\mu > 0$  in the expression  $\langle k_{nn} \rangle_i \sim k_i^\mu$  for the average degree of the neighbours of a node  $i$  as a function of the node's  $i$  degree, suggesting that the nodes of similar connectivity are mutually connected. Fig. 1b shows the assortative feature with  $\mu \sim 1.19 \pm 0.06$  for the graph of our simplicial complex. Notably, statistically similar assortative correlations are present in the degree-preserving randomised structure. Meanwhile, the random graph and the simple scale-free networks have  $\mu \sim 0$  compatible with the

absence of degree correlations. Furthermore, Fig. 1c-d shows that, in the graph's metric space (endowed with the shortest-path distance), these graphs have a relatively small diameter, and hyperbolicity or negative curvature [43, 44], precisely they are  $\delta$ -hyperbolic with a small  $\delta$  value [45, 46]. Moreover, due to the attachments among cliques[47], which are 0-hyperbolic objects, it was shown [27] that the topological graphs of the emergent assembly are always 1-hyperbolic. Practically, this means that the maximum observed  $\delta$  in the Gromov hyperbolicity criterion [45] can not exceed the value 1 for any four-tuple of nodes in that graph. In Fig. 1d we show

how the  $\delta_{max}$  can vary with the minimal distance in a large number of sampled four-tuples for all four network structures. Notably,  $\delta_{max} = 1$  for the graph of our simplicial complex, as expected, and it increases by 1/2 with the degree-preserving randomisation of edges. In the small- $\delta$  graphs, such increases of the hyperbolicity parameter are attributed [46] to the appearance of a characteristic subadjacent structure, usually a new cycle compatible with the new  $\delta$  value. Our graph's complete randomisation and the simple scale-free structure appear to possess even larger cycles, resulting in the  $\delta_{max} = 2$ . In the following two sections, we will investigate the synchronisation processes among phase oscillators interacting via edges and triangles of these networks.

### III. PHASE SYNCHRONISATION WITH THE COMPETING SIMPLEX-BASED INTERACTIONS

The phase variable is an angle in 2-dimensional space,  $\theta_i$ , associated with the network's nodes  $i = 1, 2, 3, \dots, N$ . The local interactions among these dynamical variables of the strengths  $K_q$  are provided by the network's topology elements, which are strictly related to the corresponding faces of the simplicial complex. In this work, we consider two leading interactions associated with the edges ( $q = 1$ ) and interactions among triplets located on a triangle face ( $q = 2$ ), with the strength  $K_1$  and  $K_2$ , respectively. The evolution equations given by

$$\begin{aligned} \dot{\theta}_i = & \omega_i + \frac{K_1}{k_i^{(1)}} \sum_{j=1}^N A_{ij} \sin(\theta_j - \theta_i) + \\ & + \frac{K_2}{2k_i^{(2)}} \sum_{j=1}^N \sum_{l=1}^N B_{ijl} \sin(\theta_j + \theta_l - 2\theta_i) \end{aligned} \quad (1)$$

are coupled via the two interaction terms. In particular,  $A_{ij}$  is an element of the 1-simplex adjacency matrix  $\mathbf{A}$ , such that  $A_{ij} = 1$  if nodes  $i, j$  are connected by a link, and 0 otherwise; meanwhile,  $B_{ijl}$  is an element of the 2-simplex adjacency tensor  $\mathbf{B}$ , such that  $B_{ijl} = 1$  if nodes  $i, j, l$  belong to a common 2-simplex, and 0 otherwise. The normalisation factors in eq. (1) are the respective simplex degree of a node,  $k_i^{(q)}$ , i.e. number of distinct  $q$ -simplices that node  $i$  is part of. Specifically,  $k_i^{(1)}$  is the number of 1-simplices (edges) incident on node  $i$ , and  $k_i^{(2)}$  is the number of 2-simplices (triangles) incident on node  $i$ . Thus, equal weightage is given to all the terms contributing to the sum in each interaction term. It is important to note the number of edges and the number of triangles per node in the underlying graph of our simplicial complex obey a broad (partly a power-law) distribution, cf. Fig. 1a,f. In eq. (1),  $\omega_i$  is the intrinsic frequency of the  $i$ -th oscillator, which dictates its motion when there is no interaction with other oscillators in the network. The pairwise interactions seek to reduce the difference between the phase of the  $i$ -th oscillator and each of its neighbouring oscillators when  $K_1 > 0$ . In contrast, the oscillators tend towards opposite phases when  $K_1 < 0$ . The third term, representing three-node interactions of the  $i$ -th oscillator based on each 2-simplex incident on node  $i$ , is a natural generalization of the pair-wise interaction term [10]. It should be

stressed that the interactions between these three nodes occur over faces of the simplicial complex and not over any given three nodes. Furthermore, this interaction term is symmetric in  $i$ , in that it is unaffected by permutations in the other two indices. Revealing the impact of the 2-simplex term in Eq. (1) on the synchronisation processes that are promoted by the pairwise interactions is one of the objectives of this work.

As it is widely accepted, the degree of synchronisation of the whole network is quantified by the Kuramoto order parameter

$$r = \left\langle \left| \frac{1}{N} \sum_{j=1}^N e^{i\theta_j} \right| \right\rangle, \quad (2)$$

where the brackets  $\langle \cdot \rangle$  indicate the time average. Hence,  $r = 1$  represents the perfect synchronisation, i.e., all phases are equal, and  $r = 0$  in the disordered phase. Meanwhile, the stable states with  $0 < r < 1$  indicate the presence of more complex patterns and partial synchronisation.

In the simulations, the initial conditions are set for  $\theta_i$  and  $\omega_i$  as the uniform random number in the range  $\theta_i \in [0, 2\pi]$  and the Gaussian random number with a zero mean and unit variance, respectively. The numerical solution of the set of equations (1) is performed using a numerical integrating function `odeint` from Python's SciPy library [48]. This function integrates a system of ordinary differential equations (ODEs) using the `lsoda` solver from the Fortran library ODEPACK. It solves ODEs with the Adams (predictor-corrector) method the Backward Differentiation Formula for non-stiff and stiff case, respectively. For each set of parameter values, the system is iterated for 50000 steps. The last 20000 iterations are used to calculate the order parameter as in Eq. (2). Further, in order to study hysteresis, we track the trajectory of the system as the coupling parameter  $K_1$  is first adiabatically increased and then decreased. The step size of coupling  $K_1$  is taken to be 0.1. Alternatively,  $K_2$  is varied in a suitable range, meanwhile fixing several representative  $K_1$  values, as described in the second part of sec. IV. A detailed program flow is given in the Appendix.

#### A. The case $K_2 = 0$ : Synchronisation under exclusively pairwise interactions

Before considering the competing simplex-based interactions, we will describe the synchronisation process under the pairwise interactions alone, i.e., when  $K_2 = 0$  in Eq. (1). As mentioned above, these interactions are enabled by the edges of the substrate network, which is the 1-skeleton of our 4-dimensional simplicial complex. Hence, different network features from local to global level are expected to play a role in the cooperative behaviours, depending on the interaction strength  $K_1$ . For the 4-dimensional simplicial complex, as  $K_1$  is increased from zero up to  $K_1 = 2.0$ , and we observe a continuous transition from a desynchronized state ( $r \approx 0$ ) to a completely synchronized state ( $r \approx 1$ ), see Fig. 2. On the other hand, with the negative values of  $K_1$  decreased from  $K_1 = 0$  to  $K_1 = -2.0$ , the order-parameter increases in a dif-

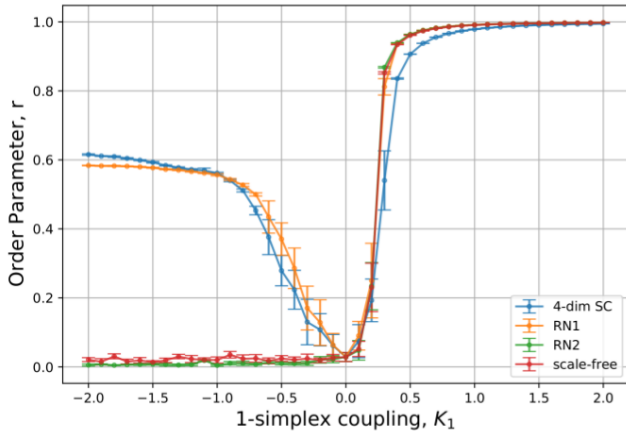


FIG. 2: The order parameter  $r$  as a function of the 1-simplex coupling strength  $K_1$  without the higher-order interactions. Calculations are plotted for 4-dimensional simplicial complex (blue), randomized network with the original degree distribution (orange), fully randomized network (green), and a simple scale-free network with the same number of nodes and edges (red).

ferent manner and reaches the value  $r \approx 0.6$ , comprising a partially synchronised state. To demonstrate what network property can be responsible for the observed synchronisation properties, we performed the simulations on the two randomised versions of the network, as described in Section II. Notably, for the degree-preserving randomised structure, RN1, qualitatively similar behaviour of the order parameter is found. In contrast, for the fully randomised network, the order parameter remains zero for all values of  $K_1 \leq 0$ . Interestingly, almost identical values of the order-parameter compatible with the absence of synchronisation at negative pairwise interactions are found in a simple scale-free network, as shown in Fig. 2. Therefore, we can conclude that the node’s assortative degree correlations in the network of our simplicial complex and in the corresponding degree-preserving randomised version, cf. Fig.1b, can be responsible for the appearance of the partial synchronisation for the negative pairwise interaction.

The distribution of phases over nodes, or the synchronisation pattern, is expected to depend on the structure. Here, the histograms of phases corresponding to different representative values of the coupling strength  $K_1$  are shown in Fig. 3 for different network structures. While the order parameter in the scale-free and entirely random network is practically identical, cf. Fig. 2, the phases in the synchronised state appear to be different, which can be attributed to the degree distribution as the only measurable difference between these networks. On the other hand, there is a remarkable similarity in the distribution of phases in the simplicial-complex network and its degree-preserving randomised version. Moreover, the peak for large positive values of  $K_1$  is close to the one seen in the corresponding scale-free structure. On the negative  $K_1$  side, the majority of phases also appear to be in the same region; see the top two rows of Fig. 3. How the partially synchronised state in these correlated networks appears is another important issue. We anticipate that a large number of triangles, as

shown in Fig. 1e, can be responsible for the frustration effects leading to the partially synchronised states in these two networks. In the following, we will examine the impact of the triangle-based interactions in our simplicial complex.

#### IV. HYSTERESIS LOOP INDUCED BY HIGHER-ORDER INTERACTIONS

In this section, we will focus attention on synchronization dynamics on our network in the presence of triangle-based interactions, i.e., using  $K_2 \neq 0$  in equation (1). We plot the time averaged order parameter  $r$  as a function of 1-simplex coupling  $K_1$ , for different 2-simplex coupling values  $K_2 = 0.0, 0.2, 0.4, 0.5, 0.8, 1.0$  in Fig. 4. In these plots, first  $K_1$  is increased adiabatically from  $K_1 = -2.0$  to  $+2.0$  (forward sweep), and then decreased from  $K_1 = +2.0$  to  $-2.0$  (backward sweep) in steps of  $dK_1 = 0.1$ . For each plot shown in Fig. 4, we see that at  $K_1 = -2$ , the system is partially synchronised, with a finite  $r$  value. The system gradually desynchronises as  $K_1$  tends towards zero. Next, as  $K_1$  is increased towards  $+2.0$ , a continuous increase of the level of synchronisation occurs. For higher values of  $K_2$ , the transition remains continuous but slows down due to possible phase-locked configurations in the region around  $K_1 \sim 0.5$ , and gradually reaches the complete synchrony at larger values of  $K_1$ . In the backward sweep, as  $K_1$  decreases from  $+2.0$  to zero and further towards  $K_1 = -2$ , the desynchronisation transition largely depends on the value of the triangle-based interactions. Namely, when  $K_2 = 0$ , the transition is continuous following the same trajectory as the forward transition, through the fully desynchronised state at  $K_1 = 0$ , and ending up with the partially synchronised state at  $K_1 = -2$ . As the coupling  $K_2$  is increased, the forward and backward transitions are no longer reversible. More precisely, when the 2-simplex interaction strengths exceeds  $K_2 \gtrsim 0.4$ , the level of synchronisation slows down in the forward sweep due to phase-locked configurations, as mentioned above. Meanwhile, in the backward sweep, we note a discontinuous desynchronisation decay towards the  $K_1 < 0$  branch. The occurrence of an abrupt desynchronisation has been previously reported in [5, 9, 10] as a prominent effect of higher-order interactions with different coupling types. In this context, the abrupt destruction of the synchronised state in our simplicial complex is also expected. What is new is the specific dependence of the hysteresis loop and thus the abrupt desynchronisation phenomenon on the strength of the 2-simplex interactions, as demonstrated by the results in Fig. 4 and Fig. 5. The abrupt transition is to a partially synchronised state with a non-zero value of the order parameter. Notably, an abrupt decay of the completely synchronised state occurs when  $K_2$  is large enough to balance the effects of the non-positive pairwise interaction  $K_1 \leq 0$ . Thus, the only complete desynchronisation transition appears at the point  $K_1 = 0$  for a small  $K_2$  value, as Fig. 4 shows. Fig. 4 shows that, beyond this value of  $K_2$ , the hysteresis loop grows in size as  $K_2$  is increased, affecting both the forward sweep at the positive  $K_1$  side and the size of the first-order jump. This scenario continues for a wider range of values of the 2-simplex inter-

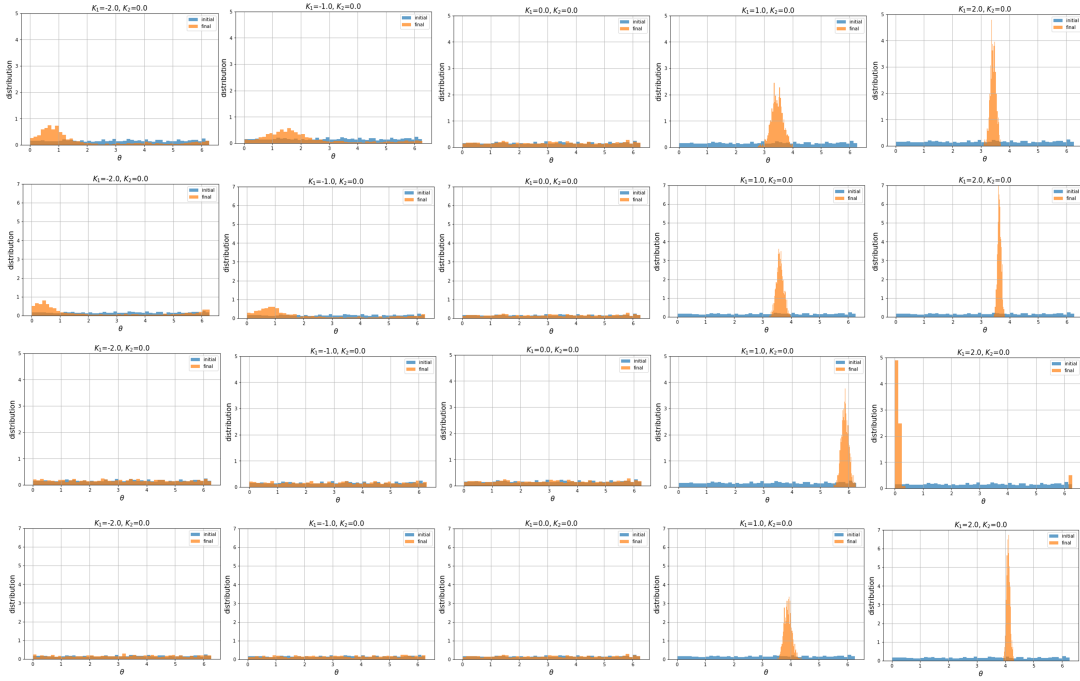


FIG. 3: Distribution of phases (measured in radians) in the initial (blue) and final (orange) states of the synchronization simulations for different values of the pairwise interaction for four network structures described in sec. II. The first row of panels is for the network of the 4-dimensional simplicial complex, the second row is for the randomized network with the original degree distribution (RN1), the third row is for the fully randomized network (RN2), and the last row is for the scale-free network with the same number of nodes and edges (SF).

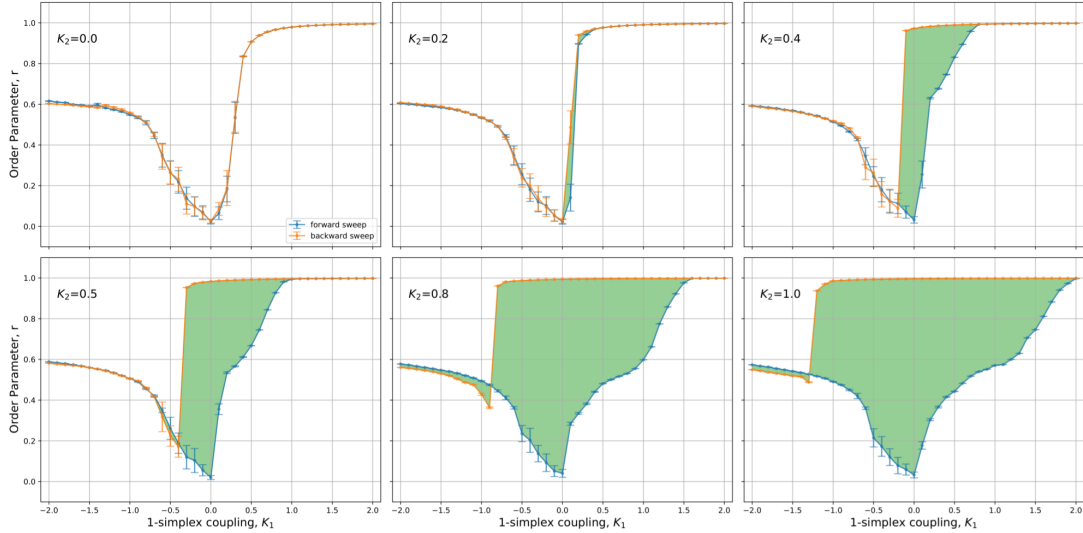


FIG. 4: Synchronization with higher-order interactions: Hysteresis sweep of the order parameter as a function of 1-simplex coupling strength  $K_1$  for different 2-simplex coupling strength  $K_2$  values. As the value of  $K_2$  increases, we notice an increase in the size of the hysteresis loop.

action strength as long as the large positive pairwise interactions are sufficient to maintain a complete synchrony. However, for larger values of  $K_2$ , the fully synchronised state is no longer accessible; instead, a kind of partially synchronisation is reached under the competing interactions. The backward sweep from such a state, as shown in Fig. 5, closes up an entirely different shape of the hysteresis loop appears with two distinct parts at positive and negative  $K_1$ , and continuous

changes of the order parameter. Hence, we can conclude that the impact of the 2-simplex encoded interactions on our 4-dimensional simplicial complex strongly depends on the sign and strength of the pairwise interactions. An overview of its effects is displayed in Fig. 6, and discussed in sec. V.

Furthermore, we analyse how the hysteresis loop area grows with increasing  $K_2$ . Particularly, we plot the area of the hysteresis loops for different values of  $K_2$  against  $K_2$

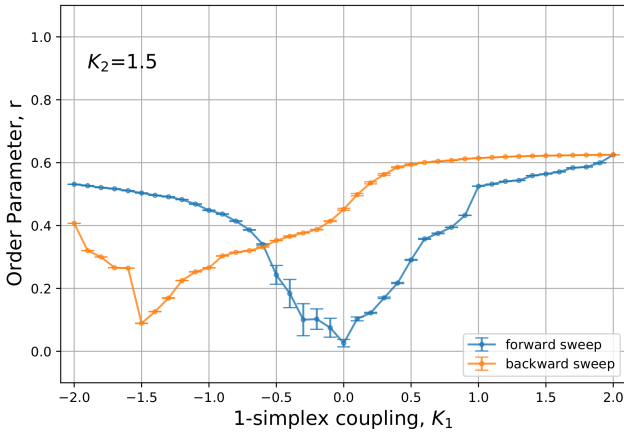


FIG. 5: Hysteresis loop for strong 2-simplex interaction  $K_2$ : only partial synchronisation is accessible even at a large positive  $K_1$ ; the abrupt desynchronisation disappears.

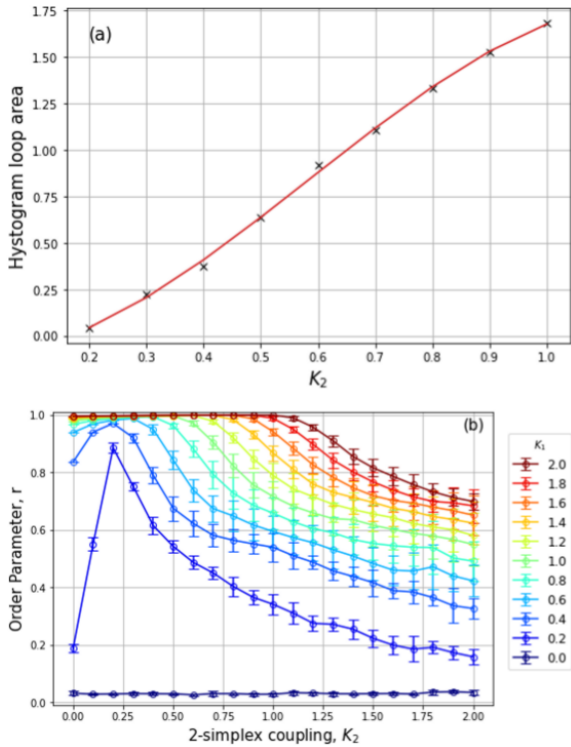


FIG. 6: (a) The size of the hysteresis loop obtained by increasing and then decreasing pairwise interaction  $K_1$ , as shown in Fig. 4, plotted against  $K_2$ ; the parameters of the cubic polynomial fit are given in the text. (b) The order parameter  $r$  against  $K_2$  for different values of  $K_1$  indicated in the legend.

in Fig. 6a. The curve is best fitted with a cubic function  $f(x) = -2.3767K_2^3 + 4.1631K_2^2 - 0.0050K_2 - 0.1043$  with root-mean-square error 0.01866.

We highlight the competing nature of the 1-simplex and 2-simplex interactions. To that end, we carry out synchronisation simulations for different pairs of coupling strengths  $K_1$  and  $K_2$ , illustrated by plotting the order parameter,  $r$ , as a func-

tion of 2-simplex coupling  $K_2$  in figure 6b. We notice that the order parameter remains negligible if the pairwise interactions are absent,  $K_1 = 0$ , for all values of  $K_2$  considered, suggesting that the 2-simplex interactions alone can not induce the system's synchronisation. Next, we notice that for finite but low values of  $K_1$ , increasing  $K_2$  leads to higher synchronisation, but only until around  $K_2 \leq 0.2$ . A further increase in  $K_2$  leads to decreasing the system's level of synchronisation, as seen from the decaying values of  $r$  with  $K_2$ . Note that higher  $K_1$  are gradually needed to compete with the desynchronising effects due to high  $K_2$ . Subsequently, the curves of  $r$  in figure 6b decrease with the increasing  $K_2$ . In this range of  $K_2$  values, the complete synchrony is no longer accessible, as also demonstrated with the hysteresis loop in Fig. 5.

## V. DISCUSSION AND CONCLUSIONS

How high-dimensional simplicial complexes can shape the dynamics is a question of great relevance to many functional systems. Among these, a prominent example is the human connectome structure underlying the brain functional complexity. To address this issue, we have studied the processes of phase synchronisation on a homogeneous 4-dimensional simplicial complex of a given size ( $10^3$  nodes); we have considered the leading interactions encoded by 1-simplex (edges) and 2-simplex (triangles) faces and varying the respective strengths  $K_1$  and  $K_2$ . Our results revealed a variety of scenarios for the synchronisation and desynchronisation (both to complete and partially desynchronised states), depending on the sign of the pairwise interactions and the geometric frustration promoted by the triangle-based interactions. The latter can be attributed to the actual organisation of 5-cliques that make the simplicial complex; notably, every link in this complex is a shared face of at least three triangles. Moreover, the geometrical properties of its underlying graph play their role. These are the assortative degree correlations, the graph's hyperbolicity, and the high spectral dimension.

More precisely, we have demonstrated that:

- the 1-simplex interactions of both signs  $K_1 \geq 0$  promote the synchronisation but with different mechanisms; no synchrony can arise due to 2-simplex interactions alone;
- for  $K_1 > 0$  the two interaction types have competing effects, and the complete synchrony can be reached for a moderate range of  $K_2$ , balanced by the increasingly stronger pairwise coupling  $K_1$ ;
- for the negative pairwise interactions  $K_1 < 0$ , however, the 2-simplex interactions support the mechanisms leading to partially ordered states due to  $K_1$ ;
- the prominent impact of the 2-simplex interactions is seen in the opening-up of the hysteresis loop and the appearance of a finite jump in the backward sweep starting from the completely synchronised state, in analogy to the abrupt desynchronisation found in other studies

[5, 9, 30]. Note that, in our case, the desynchronisation is partial following the forward branch for  $K_1 \leq 0$ , except when it occurs precisely at the point  $K_1 = 0$ ;

- eventually, for substantial 2-simplex interactions  $K_2 \gtrsim K^*$  the geometric frustration prevailed, leading to partial synchronisation even though a large positive  $K_1$  is adequate; the abrupt desynchronisation entirely disappears; on the negative  $K_1 < 0$  side, a new segment of the hysteresis loop opens up, suggesting that potentially different orderings in the frustrated synchronisation may be competing before a significant negative  $K_1$  prevails;

Our 4-dimensional simplicial complex with the simplex-encoded interactions represent an excellent example to investigate how geometry influences the synchronisation and desynchronisation processes on it. Even though the considered higher-order interactions are the leading cause of new dynamical phenomena, the collective behaviour's genesis is rooted in the pairwise interactions. Hence, certain nontrivial features of the underlying network are highly relevant.

Our study sheds new light on the competing role of simplex-embedded interactions in high-dimensional simplicial complexes, which occur in many natural dynamical systems. In this context, some outstanding questions remain for the future study. For example, one such question regards the relative importance of the order of interactions that can be embedded in a given simplicial complex. Moreover, our approach traces the ways to study the role of defect simplexes, the temporally-varying simplicial architecture and distributed weights, which can have profound effects on collective dynamic behaviours.

### Acknowledgments

B.T. acknowledge the financial support from the Slovenian Research Agency under the P1-0044 program. N.G. thanks IIT Madras for the CoE Project No. SP20210777DRMHRDDIRIIT. M.C. acknowledges the use of the computing resources at HPCE, IIT Madras.

- 
- [1] R.M. D'Souza, J. Gomez-Gardenes, J. Nagler, and A. Arenas, Explosive phenomena in complex networks. *Adv. in Phys.* 68(3), 123–133 (2019).
- [2] F. A. Rodrigues, T. K. DM. Peron, P. Ji, and J. Kurths, The kuramoto model in complex networks. *Physics Reports* 610, 1–98 (2016).
- [3] M. Boguna et al., Network geometry. *Nature Review Physics* 3, 114 (2021).
- [4] D.C. da Silva, G. Bianconi, R.A. da Costa, S. N. Dorogovtsev, and J. F. F. Mendes, Complex network view of evolving manifolds. *Physical Review E* 97, 032316 (2018).
- [5] P. S. Skardal and A. Arenas, Higher order interactions in complex networks of phase oscillators promote abrupt synchronization switching. *Communications Physics* 3(1), (2020).
- [6] F. Battiston et al. Networks beyond pairwise interactions: structure and dynamics. *Phys. Reports* 874, 1 (2020).
- [7] B. Tadić, M. Andjelković, M. Šuvakov, and G. J. Rodgers, Magnetisation processes in geometrically frustrated spin networks with self-assembled cliques. *Entropy* 22(3), 336 (2020).
- [8] B. Tadić and N. Gupte, Hidden geometry and dynamics of complex networks: Spin reversal in nanoassemblies with pairwise and triangle-based interactions. *Europhys. Lett.* 132(6), 60008 (2020).
- [9] P. S. Skardal and A. Arenas, Abrupt desynchronization and extensive multistability in globally coupled oscillator simplexes. *Phys. Rev. Lett.* 122, 248301 (2019).
- [10] X. Dai, K. Kovalenko, M. Molodyk, Z. Wang, X. Li, D. Musatov et al., D-dimensional oscillators in simplicial structures: odd and even dimensions display different synchronization scenarios. *arXiv:2010.14976v1* (2020).
- [11] A. Arenas, W. Cota, J. Gómez-Gardeñes, S. Gómez, C. Granell, J. Matamalas, et al., Modeling the spatiotemporal epidemic spreading of covid-19 and the impact of mobility and social distancing interventions. *Phys. Rev. X* 10, 041055 (2020).
- [12] J. Jonsson, *Simplicial Complexes of Graphs*. Lecture Notes in Mathematics, Springer-Verlag, Berlin, 2008.
- [13] Yi Zhao and S. Maletić, *Simplicial Complexes in Complex Systems*. WORLD SCIENTIFIC, 2021.
- [14] J. R. Beaumont and A. C. Gatrell, *An introduction to Q-analysis*. Concepts and techniques in modern geography ; no. 34. Geo Abstracts, Norwich, 1982.
- [15] B. Tadić, M. Andjelković, B. M. Boshkoska, and Z. Levnajić, Algebraic topology of multi-brain connectivity networks reveals dissimilarity in functional patterns during spoken communications. *PLOS ONE* 11(11), e0166787 (2016).
- [16] B. Tadić, M. Andjelković, and R. Melnik, Functional geometry of human connectomes. *Scientific Reports* 9, 12060 (2019).
- [17] M. Andjelković, B. Tadić, and R. Melnik, The topology of higher-order complexes associated with brain hubs in human connectomes. *Scientific Reports* 10, 17320 (2020).
- [18] Z. Moradimanesh, R. Khosrowabadi, M. Eshaghi Gordji, and G. R. Jafari, Altered structural balance of resting-state networks in autism. *Scientific Reports* 11, 1966 (2021).
- [19] S. Ikeda and M. Kotani, Materials inspired by mathematics. *Science and Technology of Advanced Materials* 17(1), 253–259 (2016).
- [20] M. Andjelković, N. Gupte, and B. Tadić, Hidden geometry of traffic jamming. *Phys. Rev. E* 91, 052817 (2015).
- [21] B. Tadić, M. Andjelković, and M. Šuvakov, The influence of architecture of nanoparticle networks on collective charge transport revealed by the fractal time series and topology of phase space manifolds. *Journal of Coupled Systems and Multiscale Dynamics* 4(1), 30–42 (2016).
- [22] G. Bianconi, C. Rahmede, and Z. Wu, Complex quantum network geometries: Evolution and phase transitions. *Phys. Rev. E* 92, 022815 (2015).
- [23] M. Chutani, N. Rao, N. Nirmal Thyagu, and N. Gupte, Characterizing the complexity of time series networks of dynamical systems: A simplicial approach. *Chaos: An Interdisciplinary Journal of Nonlinear Science* 30(1), 013109 (2020).
- [24] M. Andjelković, B. Tadić, M. Mitrović Dankulov, M. Rajković, and R. Melnik, Topology of innovation spaces in the knowledge networks emerging through questions-and-answers. *PLOS ONE* 11(5), e0154655 (2016).



- [25] U. Alvarez-Rodriguez et al., Evolutionary dynamics of higher-order interactions in social networks. *Nature Human Behaviour*, 2021.
- [26] B. Tadić, Self-organised criticality and emergent hyperbolic networks: blueprint for complexity in social dynamics. *European Journal of Physics* 40(2), 024002 (2019).
- [27] M. Šuvakov, M. Andjelković, and B. Tadić, Hidden geometries in networks arising from cooperative self-assembly. *Scientific Reports* 8, 1987 (2018).
- [28] B. Tadić, M. Šuvakov, M. Andjelković, and G. J. Rodgers, Large-scale influence of defect bonds in geometrically constrained self-assembly. *Phys. Rev. E* 102, 032307 (2020).
- [29] M. Šuvakov, M. Andjelković, and B. Tadić, Applet: Simplex aggregated growing graph (<http://suki.ipb.rs/ggraph/>). 2017.
- [30] K. Kovalenko et al., Growing scale-free simplices. *Communications physics* 4, 43 (2021).
- [31] M. Mitrović Dankulov, B. Tadić, and R. Melnik, Spectral properties of hyperbolic networks with tunable aggregation of simplexes. *Physical Review E* 100, 012309 (2019).
- [32] R. Ghorbanchian, J. Restrepo, J.J. Torres, and G. Bianconi, Higher-order simplicial synchronization of coupled topological signals. *arXiv:2011.00897v1*, 2020.
- [33] A. Arenas, A. Díaz-Guilera, J. Kurths, Y. Moreno, and C. Zhou, Synchronization in complex networks. *Physics Reports* 469(3), 93–153 (2008).
- [34] P. Li, K. Zhang, X. Xu, J. Zhang, and M. Small, Reexamination of explosive synchronization in scale-free networks: The effect of disassortativity. *Phys. Rev. E* 87, 042803 (2013).
- [35] A. P. Millán, J. J. Torres, and G. Bianconi, Synchronization in network geometries with finite spectral dimension. *Physical Review E* 99(2), 022307 (2019).
- [36] Hui Wu and Mukesh Dhamala, Dynamics of kuramoto oscillators with time-delayed positive and negative couplings. *Phys. Rev. E*, 98:032221, Sep 2018.
- [37] F. Dai, S. Zhou, T. Peron, W. Lin, and P. Ji, Interplay among inertia, time delay, and frustration on synchronization dynamics. *Phys. Rev. E* 98, 052218 (2018).
- [38] S.-Y. Ha, D. Ko, and Y. Zhang, Emergence of phase-locking in the kuramoto model for identical oscillators with frustration. *SIAM Journal on Applied Dynamical Systems* 17, 581–625 (2018).
- [39] P. Khanra, P. Kundu, C. Hens, and P. Pal, Explosive synchronization in phase-frustrated multiplex networks. *Phys. Rev. E* 98, 052315 (2018).
- [40] D. Goldstein, M. Giver, and B. Chakraborty, Synchronization patterns in geometrically frustrated rings of relaxation oscillators. *Chaos: An Interdisciplinary Journal of Nonlinear Science* 25(12), 123109 (2015).
- [41] H. Xia, G. Jian, S. Yu-Ting, Z. Zhi-Gang, and X. Can, Effects of frustration on explosive synchronization. *Frontiers of Physics* 11(6), 110504 (2016).
- [42] S. Dorogovtsev, *Lectures on Complex Networks*. Oxford University Press, Inc., New York, NY, USA, 2010.
- [43] O. Narayan and I. Sanjeev, Large-scale curvature of networks. *Phys. Rev. E* 84, 066108 (2011).
- [44] W. Chen, W. Fang, G. Hu, and M.W. Machoney, *On the hyperbolicity of small-world and tree-like random graphs*, pages 278–288, LNCS 7676, Springer-Verlag Berlin Heidelberg, 2012.
- [45] S. Bermudo, J. M. Rodríguez, J. M. Sigarreta, and J.-M. Vilaire, Gromov hyperbolic graphs. *Discrete Mathematics* 313(15), 1575–1585 (2013).
- [46] S. Bermudo, J. M. Rodríguez, O. Rosario, and J. M. Sigarreta, Small values of the hyperbolicity constant in graphs. *Discrete Mathematics* 339(12), 3073–3084 (2016).
- [47] N. Cohen, D. Coudert, G. Ducoffe, and A. Lancin, Applying clique-decomposition for computing gromov hyperbolicity. *Theoretical Computer Science* 690(Supplement C):114 – 139, 2017.
- [48] P. Virtanen, R. Gommers, T.E. Oliphant, M. Haberland, T. Reddy, D. Cournapeau, et al. *SciPy 1.0: Fundamental Algorithms for Scientific Computing in Python*. *Nature Methods* 17, 261–272 (2020)

## Appendix

### A. Program Flow

- 
- 1: INPUT Graph  $\mathcal{G}$ , stored as an list of edges and list of triangles;
  - 2: Initialize phases of the oscillators,  $\theta_i$ , such that they are distributed uniformly between 0 and  $2\pi$ ;
  - 3: Initialize intrinsic frequencies of the oscillators,  $\omega_i$ , such that they are distributed normally, with zero mean and unit variance;
  - 4: Set the value  $K_2$ . Assign  $K_2 = 0$ , if 2-simplex interactions are to be ignored. Assign finite  $K_2$ , if 2-simplex interactions are to be added;
  - 5: Set the value  $K_1 = -2.0$ ; Set the incremental change in  $K_1$  to be  $dK_1 = 0.1$ ;
  - 6: Forward sweep:
  - 7: **while**  $K_1 \leq +2.0$  **do**
  - 8:   **for all** nodes  $i \in \mathcal{G}$  **do**
  - 9:     solve the differential equation (1);
  - 10:   **end for**
  - 11:   Calculate order parameter for the system, using equation (3);
  - 12:   Increase  $K_1$  by  $dK_1$ ;
  - 13: **end while**
  - 14: Backward sweep:
  - 15: **while**  $K_1 \geq -2.0$  **do**
  - 16:   **for all** nodes  $i \in \mathcal{G}$  **do**
  - 17:     solve the differential equation (1);
  - 18:   **end for**
  - 19:   Calculate order parameter for the system, using equation (3);
  - 20:   Decrease  $K_1$  by  $dK_1$ ;
  - 21: **end while**
  - 22: END
-